Tapping Atomic Force Microscopy Imaging at Phase Resonance

Baishun Sun, Chenchen Xie, Kaige Qu, Liang Cao, Jin Yan, Ying Wang, Liguo Tian, Wenxiao Zhang, Zuobin Wang*
International Research Centre for Nano Handling and Manufacturing of China,
Changchun University of Science and Technology,
Changchun 130022, China
wangz@cust.edu.cn

Baishun Sun, Chenchen Xie, Kaige Qu, Liang Cao, Jin Yan, Ying Wang, Liguo Tian, Wenxiao Zhang, Zuobin Wang*
Ministry of Education Key Laboratory for Cross-Scale Micro and Nano Manufacturing, Changchun University of Science and Technology,
Changchun 130022, China
wangz@cust.edu.cn

Zuobin Wang*
JR3CN & IRAC, University of Bedfordshire,
Luton LU1 3JU, UK
zuobin.wang@bed.ac.uk

***Abstract*—Tapping atomic force microscope (TM-AFM) can measure soft samples, which has the advantages of low loss and high resolution, and has been widely used in the characterization of soft micro-nano materials by atomic force microscope (AFM). The phase image in TM-AFM contains sample properties, and it is an important method to characterize the sample by TM-AFM. At present, researchers usually select the frequency near the first resonance peak of the probe to drive its vibration to carry out scanning imaging. However, the phase sensitivity near the first-order resonance of the probe is not high. Therefore, the phase image of TM-AFM is also less sensitive to characterize micro-nano materials. In order to improve the phase sensitivity of the probe, the probe working at the phase resonance peak was selected in this paper to improve the phase sensitivity of the probe vibration and the imaging quality of TM-AFM phase image. The experimental results show that the phase image of phase resonance-atomic force microscope (PR-AFM) can provide not only the surface information but also the structure information of the sample subsurface. PR-AFM can be applied for better characterization of micro and nano materials.**

Keywords*— *PR-AFM, Phase image, TM-AFM, Soft sample

I. Introduction

AFM is important for the study of topography, mechanics, subsurface structure and other properties of micro and nano materials [1-5]. Therefore, AFM has aroused strong interest of researchers since its invention in 1986 [6-7]. After decades of development, many types of AFM have evolved. AFM can be basically divided into three types: contact-AFM, non-contact-AFM and TM-AFM [8]. TM-AFM not only has the same high resolution as contact-AFM, but also has less damage to the measured sample [9-10], so TM-AFM is particularly suitable for soft micro-nano materials, especially for the scientific research of microscopic biological samples [11]. As shown in Fig.1, the basic principle of TM-AFM is to make the AFM probe vibrate in the vertical direction of the sample surface with a certain amplitude and frequency of $A_D sin(\omega t)$[12]. By changing the distance $Z(x,t)$ between the AFM probe and the sample, the real-time amplitude of probe $A(x,t)$ is constant as A_{st} (the setpoint amplitude of the probe) [13-15]. The topography image, phase image and amplitude image can be obtained according to the changes of the amplitude $(A(x,t) - A_{st})$ and the changes in phase (φ) of the probe vibration [16-17].

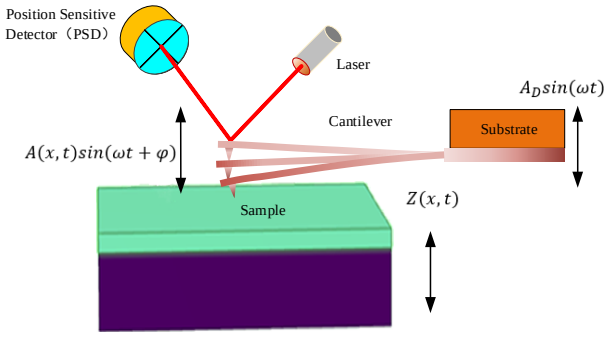

Fig. 1. TM-AFM working principle. The AFM probe vibrate in the vertical direction of the sample surface with a certain amplitude and frequency of $A_D sin(\omega t)$. By changing the distance $Z(x,t)$ between the AFM probe and the sample, the real-time amplitude of probe $A(x,t)$ is constant as A_{st}. The topography image, phase image and amplitude image can be obtained according to the changes of the amplitude $(A(x,t) - A_{st})$ and the changes in phase (φ) of the probe vibration.

The phase image in TM-AFM contains the properties of the measured sample. Therefore, TM-AFM phase imaging is an important method for micro-nano material characterization [18]. The accuracy of the phase image is determined by the phase sensitivity of the probe [19]. TM-AFM usually selects the frequency near the resonance peak of the probe amplitude to drive the probe vibration for scanning imaging. The amplitude sensitivity of the probe near the resonance peak of the probe amplitude is high, but the phase sensitivity of the probe is relatively low. In order to improve the imaging accuracy of the phase image [20], the frequency of the phase resonance peak of the probe vibration is selected to drive the probe vibration and carry out scanning imaging.

II. Method and Experiment

A. Phase resonance

The TM-AFM probe vibration system consists of a probe, a probe frame and a piezoelectric displacement device to drive the probe vibration. In addition to the main resonance of the probe vibration system, there are some non-main resonances in the probe vibration system [21-22]. In the experiment, it was found that there was a phase resonance near the non-main resonance, and the sensitivity of phase

change at some phase resonances was higher than that near the main resonance [23].

Fig. 2 shows the phase spectrum and amplitude spectrum of the TM-AFM probe near the phase resonance to the left of the first-order main resonance.

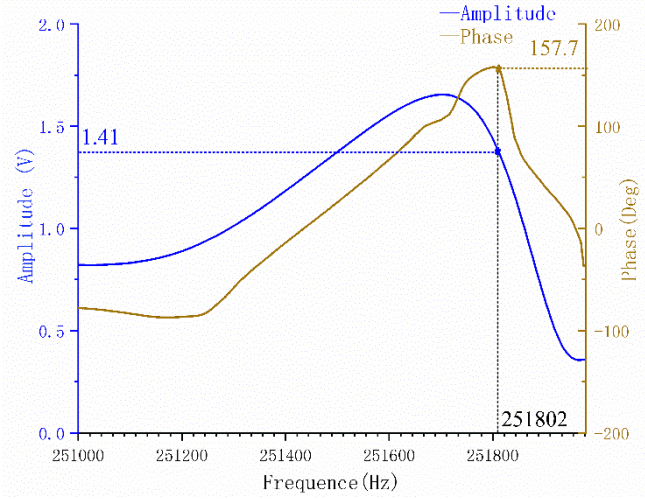

Fig. 2. Phase spectrum and amplitude spectrum of TM-AFM probe working near the phase resonance peak. The frequency at the phase resonance peak of the probe is 251802 Hz, the phase value is 157.7°, and the amplitude is 1.41 V.

B. Spin-coated photoresist sample preparation

The parameters of spin coater (KW-4, manufactured by Institute of Electronics, Chinese Academy of Sciences) were set as follows: when the rotating speed was set to 500 r/min, the spinning time was 10 s, and when the rotating speed was 3000 r/min, the spinning time was 30 s. As shown in Fig.3，in the darkroom, the spin coated photoresist SU-8-2000.5 (negative epoxy photoresist, manufactured by Micro Resist Technology GmbH, Germany) on the surface of the wafer using the spin coater. After the coating, the wafer was placed on the 95° hot plate (DB-XAB, manufactured by Shanghai Licheng BangXi Instrument Technology, China) and baked it for one minute. Through the above methods, SU8-2000.5 with the thickness of 500 nm was spin-coated on the silicon wafer with the size of 20 mm×20 mm.

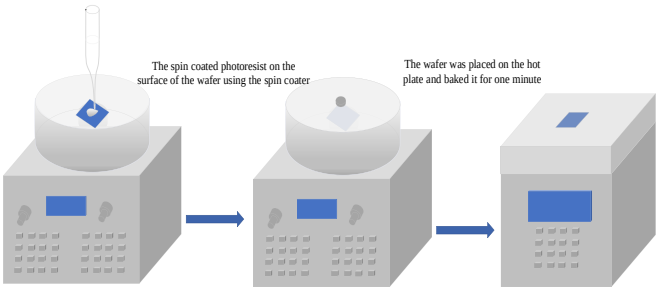

Fig. 3. Spin-coated photoresist sample preparation process. the spin coated photoresist SU-8-2000.5 on the surface of the wafer using the spin coater. After the coating, the wafer was placed on the 95° hot plate and baked it for one minute.

C. Preparation of solidified cells

Lung cancer cells (SMC-7721) were cultured in a cell incubator with 5% carbon dioxide at 37℃. As shown in Fig.4，cell platting was performed when the SMC-7721 filled the bottom of 80% the cell culture dish. The cells were placed on the cell substrates and the cells were placed in the incubator for 12 hours so that the cells were completely attached to the slide. The cell substrates were washed with phosphate buffer solution (PBS) for 2 times, and the glutaraldehyde cell curing solution with the concentration of 8% was added. The cells were placed in a refrigerator at 4℃ for 12 hours, and the excess glutaraldehyde around the cells was removed with a pipettor gun, so that the solidified cell samples were prepared.

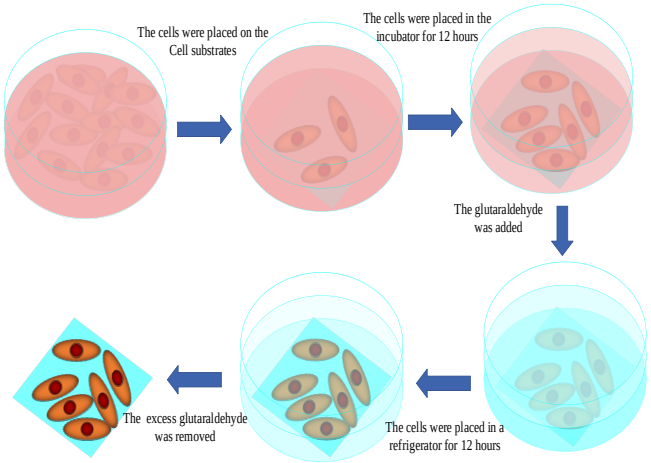

Fig. 4. Preparation of solidified cells process. The cells were placed on the cell substrates, when the cells filled the bottom of 80% the cell culture dish. The cells were placed in the incubator for 12 hours so that the cells were completely attached to the slide. The glutaraldehyde cell curing solution with the concentration of 8% was added. The cells were placed in a refrigerator at 4℃ for 12 hours, and the excess glutaraldehyde around the cells was removed with a pipettor gun, so that the solidified cell samples were prepared.

III. Results and Discussions

A. Analysis of the influence of A_{st} on PR-AFM imaging

According to the analysis of TM-AFM working principle, the magnitude of A_{st} value is the main factor that determines the change of probe vibration amplitude and phase [24]. Therefore, it is necessary to analyze the influence of A_{st} on PR-AFM imaging.

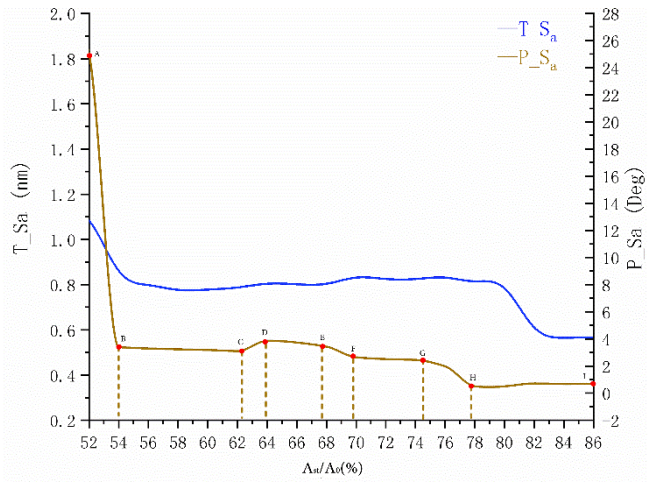

Fig. 5. Influence of the change of A_{st}/A_0 percentage value on PR-AFM imaging. The blue line is the curve of the roughness T_S_a of the topography with the change of the percentage of A_{st}/A_0. The dark yellow line is the curve of the roughness P_S_a of the phase image with the change of the percentage of A_{st}/A_0.

The TM-AFM working mode was used with the atomic force microscope of the CSPM5500 AFM (manufactured by

Benyuan Company, China). The frequency at the phase resonance peak was 251802 Hz as the driving frequency of the probe vibration, as shown in Fig. 2. The initial amplitude (A_0) of the probe was 1.41V and the initial phase was 157.7°. The scanning speed was set to 1.0 lines per second, and the image pixel size was set to 256 pixels × 256 pixels. The PR-AFM scanning imaging was performed on the spin coated SU-8-2000.5 sample by changing the A_{st}/A_0 percentage value. The roughness of the image was used to measure the influence of different A_{st}/A_0 percentage values on the PR-AFM image. The topography image roughness (T_S_a) and phase image roughness (P_S_a) were used to measure the influence of different A_{st}/A_0 percentage values on PR-AFM images (as shown in Fig. 5). When the percentage of A_{st}/A_0 varied from 54% - 80%, the range of T_S_a was about 0.8 nm-1.1 nm, and the range of P_S_a was about 0.8° - 25°. Therefore, when the percentage of A_{st}/A_0 changed within the range of 52% - 86%, it had little influence on the topography in PR-AFM, but had a significant influence on the phase in PR-AFM. This indicates that PR-AFM has almost no damage to the test samples and can be applied to the measurement of soft samples. Fig. 5 shows the topography and phase images of the sample scanned by PR-AFM at different A_{st}/A_0 percentage values, respectively. As shown in Fig. 5, the percentage of P_S_a along with A_{st}/A_0 can be roughly divided into the flat region and variation region. The areas of variations in Fig. 5 are AB, CD, EF, GH， and BC, DE, FG, HI are flat regions. This shows that the influence of some A_{st}/A_0 percentage values on the phase image is segmented. P_S_a changes with the change of A_{st}/A_0 percentage values in the variation region, while P_S_a almost does not change with the change of A_{st}/A_0 percentage values in the flat region.

B. Cell scanning imaging

The A_{st}/A_0 percent value has a significant influence on the phase image in PR-AFM, so the experiment on the scanning imaging of SMC7721 cells is carried out by changing different A_{st}/A_0 percent values. The TM-AFM working mode was used with the atomic force microscope of the CSPM5500 AFM. The frequency at the phase resonance peak was 251802 Hz as the driving frequency of the probe vibration, as shown in Fig. 2. The initial amplitude (A_0) of the probe was 1.41V and the initial phase was 157.7°. The scanning speed was set to 1.0 lines per second, and the image pixel size was set to 256 pixels × 256 pixels.

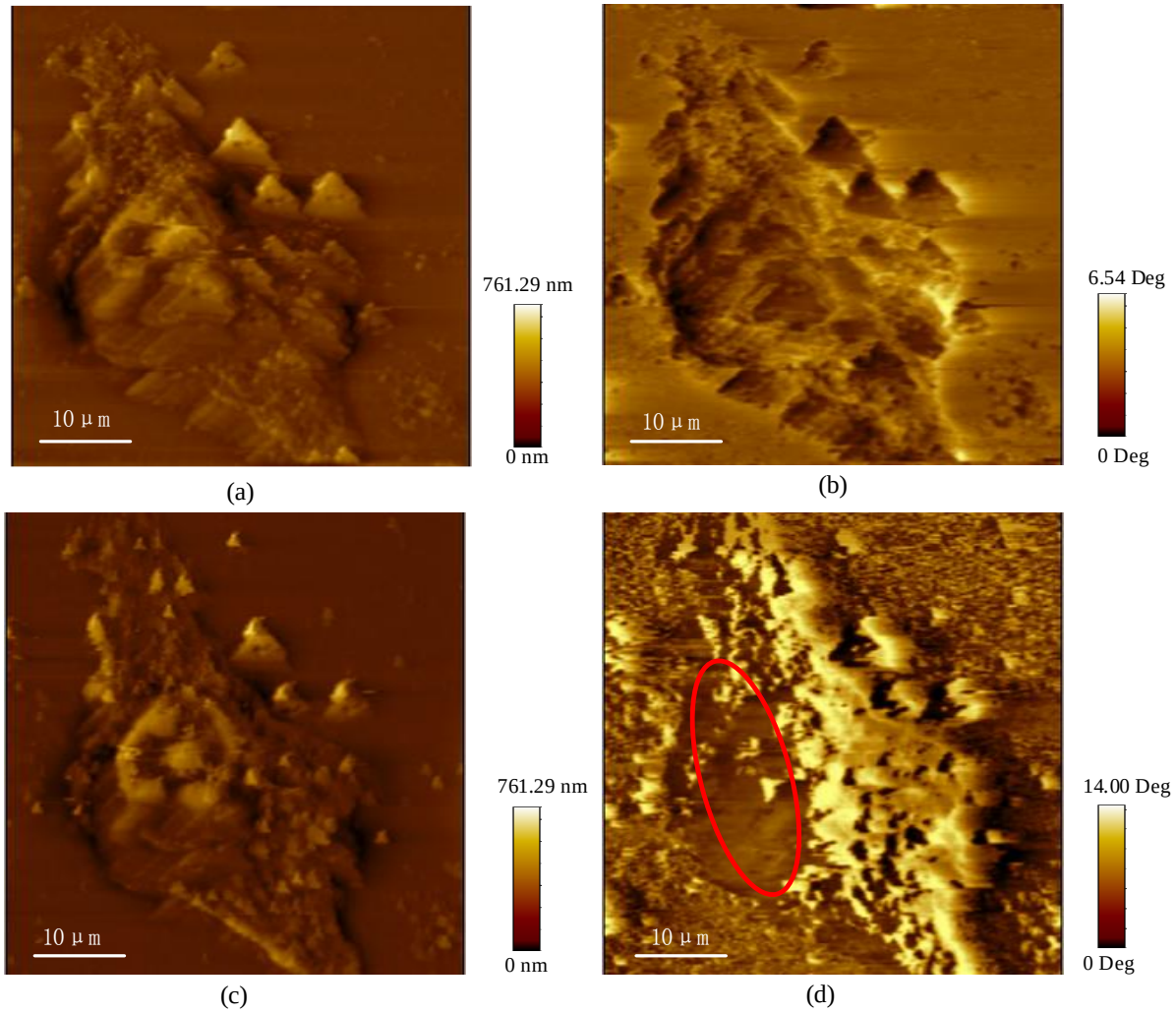

Fig. 6. PR-AFM scanning images of SMC7721 cells with different A_{st}/A_0 percentage values. (a) and (b) are the topography and phase images of SMC7721 cells with the A_{st}/A_0 percentage value of 72%. (c) and (d) are the topography and phase images of SMC7721 cells with the A_{st}/A_0 percentage value of 54%. The structure at the bottom of the cell can be seen in the left red area of the phase image (d).

In the experiment, the AFM was used for the PR-AFM imaging of SMC7221 with the A_{st}/A_0 percentages of 72% and 54% set as the above scanning parameters. As shown in Fig. 6, (a) and (b) are the topography and phase images of

SMC7721 cells with the A_{st}/A_0 percentage value of 54%. (c) and (d) are the topography and phase images of SMC7721 cells with the A_{st}/A_0 percentage value of 54%. The topography images (a) and (c) have little change, while the phase images (b) and (d) have significant changes, which are consistent with the theory in Section 3.1 that the percentage of A_{st}/A_0 has little influence on the topography image of PR-AFM, but have significant influences on the phase image. The structure at the bottom of the cell can be seen in the left red area of the phase image (d), indicating that PR-AFM can be used for the study of subsurface imaging of the sample.

IV. Conclusion

In summary, PR-AFM is an AFM imaging method which uses TM-AFM to select the frequency working at the phase resonance peak of the probe vibration to drive the probe to scan and image the test sample. By setting different percentage values of A_{st}/A_0, the PR-AFM scanning imaging was carried out on the SU8-2000.5 samples with the spin-coated thickness of 500 nm. It was found that when the percentage value of A_{st}/A_0 was 52% - 86%, the percentage value had little influence on the topography of PR-AFM, and the phase image of PR-AFM was significantly affected. This indicates that PR-AFM has almost no damage to the test samples and can be applied to the measurement of soft samples.

The PR-AFM scanning imaging of SMC7721 cells was carried out with the percentage values (A_{st}/A_0) of 54% and 72%, respectively. It was found that the topographies of the two cells changed little, but the phase pattern changed significantly. The bottom structure of SMC7721 cells was observed in the phase image with the percentage of 54%. This indicates that PR-AFM can perform subsurface imaging of the sample. The experimental results show that the phase image of PR-AFM can provide not only the surface information but also the structure information of the sample subsurface. Thus, PR-AFM is a useful tool for the scanning imaging of micro and nano materials with high phase sensitivity and can carry out the subsurface measurement.

Acknowledgment

This work was supported by National Key R&D Program of China (No. 2017YFE0112100), EU H2020 Program (MNR4SCell No. 734174; NanoStencil No. 767285), Jilin Provincial Science and Technology Program (Nos. 2020C022-1, 20190201287JC, 20190702002GH and 20200901011SF), Jilin Province Education Department Program (Nos. JJKH20210833KJ), and “111” Project of China (No. D17017).

References

[1] D. Georgakaki, S. Mitridis, A. A. Sapalidis, E. Mathioulakis, and H. M. Polatoglou, "Calibration of tapping AFM cantilevers and uncertainty estimation: Comparison between different methods," Measurement, vol. 46, pp. 4274–4281, 2013.

[2] M. Basso, P. Paoletti, B. Tiribilli, and M. Vassalli, “Modeling and analysis of auto-tapping AFM,” in 2008 47th IEEE Conference on Decision and Control, Cancun, Mexico, pp. 5188–5193, 2008.

[3] M. H. Yen, Y. H. Chen, Y. S. Liu, and O. K. S. Lee, "Alteration of Young’s modulus in mesenchymal stromal cells during osteogenesis measured by atomic force microscopy," Biochemical and Biophysical Research Communications, vol. 526, pp. 827–832, 2020.

[4] G. Krämer, M. Griepentrog, E. Bonaccurso, and B. Cappella, "Study of morphology and mechanical properties of polystyrene–polybutadiene blends with nanometre resolution using AFM and force–distance curves," European Polymer Journal, vol. 55, pp. 123–134, 2014.

[5] X. Chang, S. Hallais, S. Roux, and K. Danas, "Model reduction techniques for quantitative nano-mechanical AFM mode," Meas. Sci. Technol., vol. 32, 2021.

[6] R. W. Stark, T. Drobek, and W. M. Heckl, "Tapping-mode atomic force microscopy and phase-imaging in higher eigenmodes," Appl. Phys. Lett., vol. 74, pp. 3296–3298, 1999.

[7] Y. F. Dufrêne, A. Toshio, G. Ricardo, A. David, M. M. David, E. Andreas, G. Christoph, and J. M. Daniel, "Imaging modes of atomic force microscopy for application in molecular and cell biology," Nature Nanotech, vol. 12, pp. 295–307, 2017.

[8] V. Settimi and G. Rega, "Influence of a locally-tailored external feedback control on the overall dynamics of a non-contact AFM model," International Journal of Non-Linear Mechanics, vol. 80, pp. 144–159, 2016.

[9] M. Okada, I. Masayuki, M. Hiroto, O. Takeshi, H. Yuichi, K. Kazuhiro, and M. Shinji, "Evaluation of oxygen inhibition for UV-curable resins by adhesion force measurement using scanning probe microscope," J. Vac. Sci. Technol. B., Vol. 28, pp. C6M17-C6M22, 2010.

[10] M. Bramowicz, S. Kulesza, and K. Rychlik, "A Comparison between Contact and Tapping AFM Mode in Surface Morphology Studies," Technical Sciences, Vol.15, pp.307-318, 2012.

[11] Y.F. Dufrene, M. D. Martinez, I. Medalsy, D. Alsteens D, D.J. Muller, "Multiparametric imaging of biological systems by force-distance curve-based AFM, " Nat Methods, vol. 10, pp. 847–854,2013.

[12] S. Belikov and S. Magonov, "Modeling of Cantilever Beam under Dissipative and Nonlinear Forces with Application to Multi-Resonant Atomic Force Microscopy," IFAC, vol. 50, pp. 8654–8661, 2017.

[13] D. Forchheimer, R. Forchheimer, and D. B. Haviland, "Improving image contrast and material discrimination with nonlinear response in bimodal atomic force microscopy," Nat Commun., vol. 6, 2015.

[14] C. Su, L. Huang, K. Kjoller, and K. Babcock, "Studies of tip wear processes in tapping mode atomic force microscopy," Ultramicroscopy, vol. 97, pp. 135–144, 2003.

[15] N. F. Martínez and R. García, "Measuring phase shifts and energy dissipation with amplitude modulation atomic force microscopy," Nanotechnology, vol. 17, pp. S167–S172, 2006.

[16] J. Skibinski, J. Rebis, L. Kaczmarek, T. Wejrzanowski, T. Plocinski, and K. Rozniatowski, "Phase imaging quality improvement by modification of AFM probes’ cantilever," Journal of Microscopy, vol. 269, no. 3, pp. 179–186, 2018.

[17] S. Hu and A. Raman, "Analytical formulas and scaling laws for peak interaction forces in dynamic atomic force microscopy," Appl. Phys. Lett., vol. 91, pp. 123106, 2007.

[18] B. Xue, Y. Yan, Z. Hu, and X. Zhao, "Study on effects of scan parameters on the image quality and tip wear in AFM tapping mode: Study on the tip wear of AFM," Scanning, vol. 36, pp. 263–269, 2014.

[19] M. Sajjadi, H. N. Pishkenari, and G. Vossoughi, "Finite element modeling of trolling-mode AFM," Ultramicroscopy, vol. 189, pp. 24–38, 2018.

[19] M. J. Minary and M.-F. Yu, "Nanomechanical imaging of soft samples in liquid using atomic force microscopy," J. Appl. Phys., vol. 114, 2013

[20] A. Phani, H. S. Jung, and S. Kim, "Deconvolution of dissipative pathways for the interpretation of tapping-mode atomic force microscopy from phase-contrast," Commun Phys., vol. 4, 2021.

[21] H. Nagao, T. Uruma, K. Shimizu, N. Satoh, and K. Suizu,"Non-resonant frequency components observed in a dynamic Atomic Force Microscope," NOLTA, vol. 8, pp. 118–128, 2017.

[22] A. Sebastian, A. Gannepalli, and M. V. Salapaka, "A Review of the Systems Approach to the Analysis of Dynamic-Mode Atomic Force Microscopy," IEEE Trans. Contr. Syst. Technol., vol. 15, pp. 952–959, 2007.

[23] R. García and A. San Paulo, "Dynamics of a vibrating tip near or in intermittent contact with a surface," Phys. Rev. B., vol. 61, pp. 13381–13384, 2000.

[24] B. Gotsmann, H. Fuchs, "Dynamic force spectroscopy of conservative and dissipative forces in an Al-Au(111) tip–sample system," Phys. Rev. Lett., vol. 86, pp. 2597–2600, 2001.